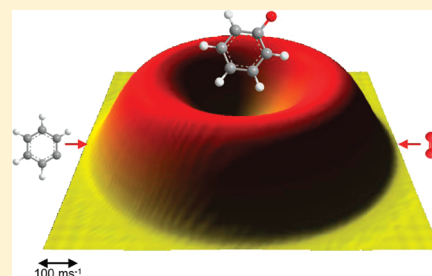


# Phenoxy Radical ( $C_6H_5O$ ) Formation under Single Collision Conditions from Reaction of the Phenyl Radical ( $C_6H_5$ , $X^2A_1$ ) with Molecular Oxygen ( $O_2$ , $X^3\Sigma_g^-$ ): The Final Chapter?

Dorian S. N. Parker, Fangtong Zhang, and Ralf I. Kaiser\*

Department of Chemistry, University of Hawaii at Manoa, Honolulu, Hawaii 96822-2275, United States

**ABSTRACT:** The combustion relevant elementary reaction of photolytically generated phenyl radicals ( $C_6H_5$ ,  $X^2A_1$ ) with molecular oxygen to form the phenoxy radical ( $C_6H_5O$ ) plus a ground state oxygen atom was investigated under single collision conditions at a collision energy of  $21.2 \pm 0.9 \text{ kJ mol}^{-1}$ . The reaction was found to proceed indirectly via the involvement of a long-lived phenylperoxy radical ( $C_6H_5O_2$ ) intermediate that decomposed via a rather loose exit transition state. In comparison with crossed beams data obtained previously at elevated collision energies, we suggest that, as the collision energy rises from 21 to  $107 \text{ kJ mol}^{-1}$ , the lifetime of the  $C_6H_5O_2$  reaction intermediate decreases, that is, a classical behavior within the osculating complex model.



## 1. INTRODUCTION

During the past decade, the oxidation of the phenyl radical ( $C_6H_5$ ,  $X^2A_1$ ), has received considerable attention from the reaction dynamics and from the combustion chemistry communities.<sup>1–3</sup> Here, aromatic molecules such as benzene ( $C_6H_6$ ),<sup>4,5</sup> the phenyl radical ( $C_6H_5$ ),<sup>2,6</sup> and possibly *ortho*-benzynes (*o*- $C_6H_4$ )<sup>1,7</sup> are key constituents of hydrocarbon-based combustion flames. These molecules are suggested to be readily formed in combustion processes through reaction of transient  $C_3H_x$  ( $x = 2, 3$ ) and  $C_{2,4}H_x$  ( $x = 1–4$ ) radicals,<sup>8–13</sup> as well as being used directly as fuel additives (benzene) due to their high energy density and antiknocking properties.<sup>5</sup> The formation of these monocyclic aromatic species is closely linked to the origin of polycyclic aromatic hydrocarbons (PAHs) and soot in combustion systems.<sup>14</sup> Both PAHs and soot are unwanted byproducts of combustion processes and present considerable health risks.<sup>15,16</sup> The formation of PAHs is thought to involve molecular growth processes facilitated by the sequential addition of acetylene molecules ( $C_2H_2$ ) to phenyl radicals followed by cyclization.<sup>17,18</sup> However, the oxidation and, hence, removal of phenyl radicals from these reactions presents a competing process to soot formation.<sup>19</sup> Electronic structure calculations predict that at temperatures higher than 1000 K, the reaction of phenyl with molecular oxygen becomes dominant and proceeds via a rovibrationally excited phenylperoxy radical [ $C_6H_5O_2$ ]\* intermediate as an initial addition complex; the latter was inferred to emit an oxygen atom in the ground electronic state to form the phenoxy radical ( $C_6H_5O$ ).<sup>20–23</sup> Competing exit channels involve hydrogen emission to form *ortho* or *para* benzoquinone, carbon dioxide ( $CO_2$ ) emission to cyclopentadienyl ( $C_5H_5$ ), and carbon monoxide formation (CO) to yield pranyl ( $C_5H_5O$ ).<sup>20–23</sup>

Two recent crossed molecular beam experiments provided compelling evidence that, at collision energies of  $64^{24}$  and  $107 \pm 6 \text{ kJ mol}^{-1}$ ,<sup>25</sup> the reaction of molecular oxygen with phenyl radicals leads to the formation of the phenoxy radical ( $C_6H_5O$ )

plus ground state atomic oxygen ( $O(^3P_1)$ ) under single collision conditions. Albert et al. suggested that, at  $64 \text{ kJ mol}^{-1}$ , the reaction dynamics involve a phenylperoxy radical whose lifetime is longer than its rotational period; this reaction intermediate ejects an oxygen atom via a simple bond rupture process. On the other hand, Gu et al. suggested that, at an elevated collision energy of  $107 \pm 6 \text{ kJ mol}^{-1}$ , the phenylperoxy radical was rather short-lived. Here, we present a crossed molecular beam study of the reaction of phenyl radicals with molecular oxygen and the inherent formation of the phenoxy radical at a collision energy of  $21.2 \pm 0.9 \text{ kJ mol}^{-1}$ , incorporating a full error analysis, which was not conducted at a collision energy of  $64 \text{ kJ mol}^{-1}$ , and record ample TOF spectra closer toward the primary phenyl radical beam generated via photolysis of the helium-seeded chlorobenzene precursor. These data are discussed in context with Gu et al. and Albert et al.'s data obtained at higher collision energies to gain a coherent understanding of the formation of the phenoxy radical under single collision conditions.

To adequately map polyatomic potential energy surfaces theoretically, they should be explored at multiple collision energies experimentally. Having a description of the PES at more than one energy significantly aids in honing these models. Because such a large discrepancy exists between the two previous experiments, where both use different techniques for radical generation of photolysis versus pyrolysis, we revisit the problem to see how the dependence on collision complex lifetime and therefore rate constants depend on the collision energy. The most recent crossed molecular beam investigation used VUV ionization to detect the absolute reaction yields of the product channel compared to the use of impact ionization in this investigation

Received: June 29, 2011

Revised: August 31, 2011

Published: September 08, 2011

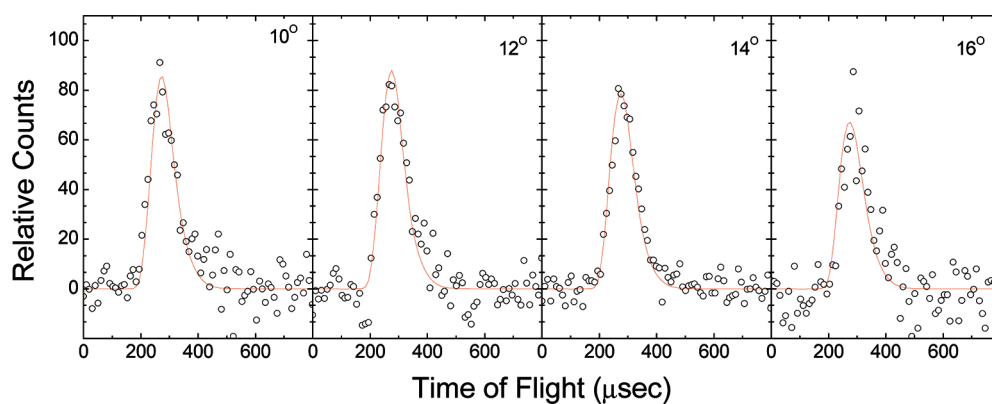


**Figure 1.** Time-of-flight data for the reaction of the phenyl radical ( $C_6H_5$ ) with molecular oxygen ( $O_2$ ) monitored at  $m/z = 93$  ( $C_6H_5O^+$ ).

and the first high energy experiment. This investigation aims to ascertain whether the discrepancies are influenced by different detection techniques and radical generation sources.

## 2. EXPERIMENTAL METHODS

The experiments were carried out under single collision conditions in a crossed molecular beams machine at the University of Hawaii.<sup>26</sup> Briefly, a molecular beam of phenyl radicals ( $C_6H_5$ ,  $X^2A_1$ ) seeded in helium (99.9999%; Gaspro) at fractions of about 1% was prepared by photolysis of chlorobenzene ( $C_6H_5Cl$  99.9%; Fluka) in the primary source. The mixture of the helium carrier gas and chlorobenzene vapor was introduced to the piezoelectric pulsed valve (Proch-Trickl) operated at a rate of 120 Hz and a backing pressure of about 1.5 atm. The chlorobenzene was photolyzed by focusing the 193 nm excimer laser output operating at 60 Hz and with a peak power of 10 mJ per pulse 1 mm downstream of the nozzle prior to the skimmer. Under our experimental conditions, the photolysis of chlorobenzene was about 90% using a  $1 \times 3$  mm focal region with an absorption cross section of  $9.6 \times 10^{-18} \text{ cm}^{-2}$  at 193 nm.<sup>27</sup> The molecular beam entraining the phenyl radical passed a skimmer and a four-slot chopper wheel, which selected a segment of the pulsed phenyl radical beam of a well-defined peak velocity ( $v_p$ ) of  $1658 \pm 12 \text{ ms}^{-1}$  and speed ratio ( $S$ ) of  $9.0 \pm 1.0$ . The radical beam bisected a pulsed molecular beam of the neat molecular oxygen generated in the secondary source with a pulsed valve at a backing pressure of 550 Torr fired 18  $\mu\text{s}$  prior to the pulsed valve in the primary source. The primary beam intersected the secondary beam at its peak intensity which corresponds to a velocity of  $776 \pm 20 \text{ ms}^{-1}$  and speed ratio of  $17.4 \pm 1.0$ , resulting in a collision energy of  $21.2 \pm 0.9 \text{ kJ mol}^{-1}$  and a center-of-mass angle,  $\Theta_{CM}$ , of  $12.0 \pm 0.7^\circ$ . The reaction products were monitored using a triply differentially pumped quadrupole mass spectrometer (QMS) in the time-of-flight (TOF) mode after electron-impact ionization of the neutral molecules at 80 eV with an emission current of 2 mA. These charged particles were separated according to their mass-to-charge ratio by an Extrel QC 150 quadrupole mass spectrometer operated with an oscillator at 1.2 MHz; only ions with the desired mass-to-charge,  $m/z$ , value passed through and were accelerated toward a stainless steel “door knob” target coated with an aluminum layer and operated at a voltage of  $-22.5 \text{ kV}$ . The ions hit the surface and initiated an electron cascade that was accelerated by the potential until they reached an aluminum-coated organic scintillator whose photon cascade was detected by a photomultiplier operated at  $-1.35 \text{ kV}$ .

The signal from the PMT was then filtered by a discriminator set to 1.6 mV prior to feeding into a Stanford Research System SR430 multichannel scaler to record time-of-flight spectra.<sup>28,29</sup> TOF spectra were recorded over the angular distribution in batches of 51120 TOFs with a total of  $\sim 2.6 \times 10^5$  TOF spectra recorded at each angle, that is, a total data accumulation time of about 70 min per angle. The TOF spectra recorded at each angle and the product angular distribution in the laboratory frame (LAB) were fit with Legendre polynomials using a forward-convolution routine.<sup>30,31</sup> This method uses an initial choice of the product translational energy  $P(E_T)$  and the angular distribution  $T(\theta)$  in the center-of-mass reference frame (CM) to reproduce TOF spectra and a product angular distribution. The TOF spectra and product angular distribution obtained from the fit were then compared to the experimental data. The parameters  $P(E_T)$  and  $T(\theta)$  were iteratively optimized until the best fit was reached. The product flux contour map,  $I(\theta, u) = P(u) \times T(\theta)$ , reports the intensity of the reactively scattered products ( $I$ ) as a function of the CM scattering angle ( $\theta$ ) and product velocity ( $u$ ). This plot is called the reactive *differential cross section* and gives an *image* of the chemical reaction.

## 3. RESULTS AND DISCUSSION

We conducted our crossed molecular beam study at a low collision energy of  $21.2 \pm 0.9 \text{ kJ mol}^{-1}$  by crossing a beam of helium-seeded, photolytically generated phenyl radicals with a second beam of neat oxygen molecules perpendicularly. Scattering signal was recorded at a mass-to-charge ratio,  $m/z$ , of 93 ( $C_6H_5O$ ). Selected time-of-flight (TOF) spectra recorded at  $m/z$  93 corresponding to the formation of the phenoxy radical plus oxygen are shown in Figure 1. The laboratory angular distribution (LAB) for all angles is shown in Figure 2. The center-of-mass angle was at  $12^\circ$ , allowing three angles in  $2^\circ$  steps to be recorded in the forward direction; however, angle  $6^\circ$  had large fluctuations in intensity due to being close to the primary beam. It should be noted that for all spectra recorded a background signal caused by elastic scattering had to be subtracted from the spectra at angles closer to the primary beam. The background signal, as verified also by nonreactive scattering experiments with molecular nitrogen in the secondary beam, decayed almost exponentially from angles 6 to  $12^\circ$  where it was below 3% of the reactive scattering signals peak area. A time-of-flight profile was recorded for each of the angles 6, 8, 10, and  $12^\circ$  for the reactive scattering signal between phenyl radicals and molecular nitrogen. In addition, the reactive scattering experiments were conducted with a 60 Hz

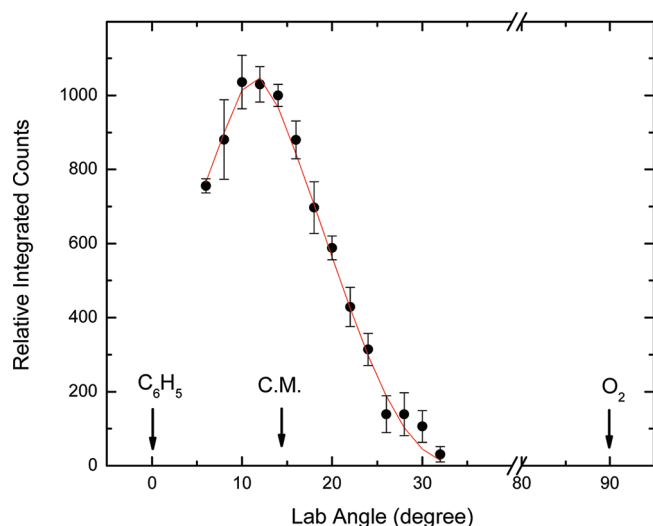


**Figure 2.** Laboratory angular distribution of the phenoxy radical ( $C_6H_5O$ ) product recorded at  $m/z = 93$  formed via the reaction of the phenyl radical ( $C_6H_5$ ) with molecular oxygen ( $O_2$ ). Circles signify experimental data, red line denotes best fit data; C.M. designates center-of-mass angle.

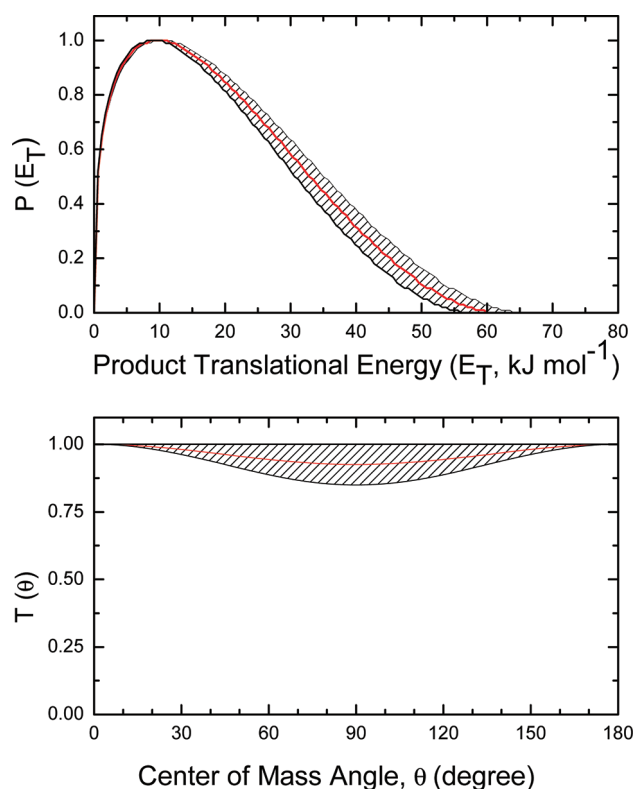


**Figure 3.** Center-of-mass translational energy flux distribution (upper) and angular distribution (lower) utilized to fit the data at  $m/z = 93$  in the reaction of phenyl radical with molecular oxygen. Hatched gray areas indicate the acceptable upper and lower error limits of the fits and the solid red line defines the best-fit function.

laser repetition rate of the laser and 120 Hz for the pulsed valve. This allowed a “laser on” minus “laser off” background subtraction of the nonreactive scattering signal as well. Once the lower angles had been processed all TOF spectra and LAB data

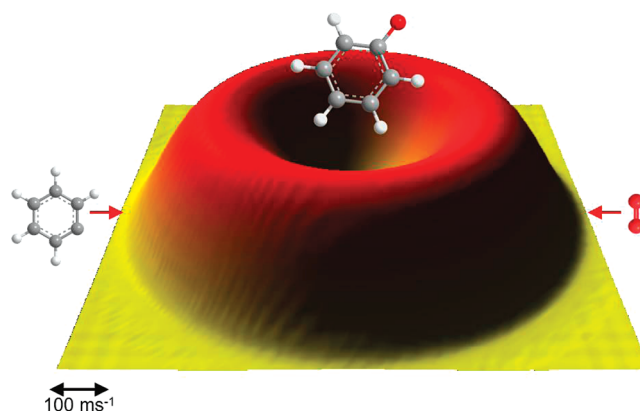


**Figure 4.** Flux contour map of the phenoxy radical ( $C_6H_5O$ ) formed in the reaction of phenyl radicals with molecular oxygen at a collision energy  $21.2 \pm 0.9 \text{ kJ mol}^{-1}$ .

(Figures 1 and 2) were able to be fit with a single channel with a mass combination of  $C_6H_5O$  (93 amu) and  $O$  (16 amu).

The corresponding center-of-mass functions are depicted in Figures 3 and 4. Here, the translational energy distribution was found to peak only slightly away from zero at about  $10 \text{ kJ mol}^{-1}$  suggesting a rather loose exit transition state. The best fits of the LAB distribution and TOF spectra were obtained with  $P(E_T)$ s extending to  $60 \pm 10 \text{ kJ mol}^{-1}$ . Because this high energy cutoff represents the sum of the collision energy ( $21.2 \pm 0.9 \text{ kJ mol}^{-1}$ ) plus the absolute of the reaction exoergicity, we can extract a reaction energy of  $-39 \pm 11 \text{ kJ mol}^{-1}$ . This agrees well with the theoretically predicted reaction energy of  $-38 \pm 8 \text{ kJ mol}^{-1}$ .<sup>25</sup> Further, the fraction of energy released into the translational degrees of freedom of the products is approximately  $28 \pm 5\%$ , that is, suggesting rather indirect scattering dynamics.<sup>32</sup> The corresponding center-of-mass angular distribution is shown in Figure 3. Best fits of the laboratory data could be obtained with functions forward–backward symmetric with respect to  $90^\circ$  and with a pronounced minimum at  $90^\circ$ . The forward–backward symmetry suggests not only indirect scattering dynamics involving a  $C_6H_5O_2$  intermediate, but also that the lifetime of the decomposing  $C_6H_5O_2$  radical is longer than its rotational period. Note that within the error limits, an isotropic distribution leads to a slightly worse fit based on the derived  $\chi^2$  analysis.

It is important to compare these findings with previous experiments of Albert et al. and Gu et al. conducted at higher collision energies of  $64 \text{ kJ mol}^{-1}$ <sup>24</sup> and  $107 \pm 6 \text{ kJ mol}^{-1}$ .<sup>25</sup> Davis communicated that the laboratory data could also be reproduced with a *forward* scattered distributions depicting a dip at  $90^\circ$ , but with intensity ratios at the poles,  $I(0^\circ)/I(180^\circ)$ , of 1.25.<sup>33</sup> The current experiment indicates an exit barrier of  $10 \text{ kJ mol}^{-1}$  matching that obtained in the mid-energy range experiment. The lack of TOF data beyond the center-of-mass angle in Gu et al.’s study closer to the primary beam and a refit of the data via a combined point and parameter form suggests that an incorporation of flux at the center-of-mass angles from  $70$  to  $180^\circ$  at levels of up to  $I(0^\circ)/I(180^\circ) \sim 9$  can still present an acceptable fit of the laboratory data. Figure 5 shows the relationship between the collision complex lifetime against the collision energy of the three experiments conducted using the new fits to the highest energy data with the pyrolytic source and the extents of the error boundaries for the middle energy from the photolytic source. Based on these considerations, we may suggest that as the

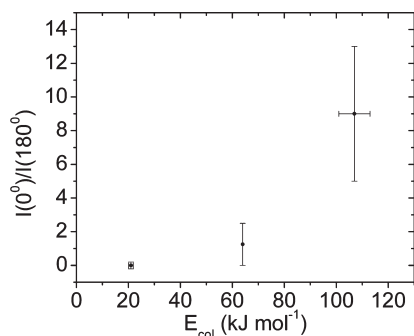


**Figure 5.** Plot of relative intensity at the poles of the center-of-mass angular distribution  $I(0^\circ)/I(180^\circ)$  vs the collision energy  $E_{col}$  (kJ mol<sup>-1</sup>).

collision energy rises from 21 to 107 kJ mol<sup>-1</sup>, the lifetime of the C<sub>6</sub>H<sub>5</sub>O<sub>2</sub> reaction intermediate decreases as the collision energy rises, that is, a classical behavior within the osculating complex model. The energy dependence indicates that the three experiments are consistent with each other and goes some way in reassuring the molecular dynamics community that the use of VUV ionization versus hard electron ionization and pyrolytic versus photolytic radical generation sources makes marginal differences in the reaction dynamics obtained. However, this is an ongoing question as to whether the differences in ionization cross section for different product channels using the VUV technique will affect branching ratios.

#### 4. CONCLUSIONS

Based on the considerations detailed above, we can conclude that at a collision energy of  $21.2 \pm 0.9$  kJ mol<sup>-1</sup>, the reaction of the phenyl radical with molecular oxygen leads to the formation of the phenoxy radical plus ground state atomic oxygen via indirect scattering dynamics involving a long-lived C<sub>6</sub>H<sub>5</sub>O<sub>2</sub> intermediate, which decomposes via a rather loose exit transition state. This loose exit transition state is in line with previous electronic structure calculations predicting that the reversed reaction of ground state oxygen with the phenoxy radical leads to a shallow van-der-Waals complex located about 5 kJ mol<sup>-1</sup> below the phenoxy radical plus atomic oxygen.<sup>21–23</sup> This complex isomerizes via a submerged barrier only ~2 kJ mol<sup>-1</sup> higher in energy compared to the van-der-Waals complex to the phenylperoxy radical, C<sub>6</sub>H<sub>5</sub>O<sub>2</sub>, residing in a deep potential energy well of about 194 kJ mol<sup>-1</sup>.<sup>21–23</sup> With the two previous experiments owning clearly different results, as described in detail by Davis et al., questions have arisen as to the reasons whether it is due to differing radical sources or from differing detection techniques. With the reworking of our previous data within the error limits established, we can see that all three experiments give results in line with each other, that the differing sources and detection techniques are still giving accurate descriptions of the reaction dynamics. The experimental measurements at different collision energies are also important to the theoretical community because they can match their diffusion coefficients at multiple energies above the zero point minimum on the PES. This represents a new trend in the relationship between theory and experiment where the mapping of the PES has multiple reference points requiring an increase in accuracy of the models to fit experimental data.

#### ACKNOWLEDGMENT

This work was supported by the U.S. Department of Energy, Basic Energy Sciences (DE-FG02-03ER15411 to the University of Hawaii).

#### REFERENCES

- (1) Vourliotakis, G.; Skevis, G.; Founti, M. A. *Energy Fuels* **2011**, *25*, 1950–1963.
- (2) Frank, P.; Herzler, J.; Just, T.; Wahl, C. *Symp. (Int.) Combust., [Proc.]* **1994**, *25th*, 833–840.
- (3) Alzueta, M. U.; Glarborg, P.; Dam-Johansen, K. *Int. J. Chem. Kinet.* **2000**, *32*, 498–522.
- (4) Defoeux, F.; Dias, V.; Renard, C.; Van Tiggelen, P. J.; Vandooren, J. *Proc. Combust. Inst.* **2005**, *30*, 1407–1415.
- (5) Yang, B.; Li, Y.; Wei, L.; Huang, C.; Wang, J.; Tian, Z.; Yang, R.; Sheng, L.; Zhang, Y.; Qi, F. *Proc. Combust. Inst.* **2007**, *31*, 555–563.
- (6) Richter, H.; Howard, J. B. *Prog. Energy Combust. Sci.* **2000**, *26*, 565–608.
- (7) Zhang, F.; Parker, D.; Kim, Y. S.; Kaiser, R. I.; Mebel, A. M. *Astrophys. J.* **2011**, *728*, 141/141–141/110.
- (8) Pope, C. J.; Miller, J. A. *Proc. Combust. Inst.* **2000**, *28*, 1519–1527.
- (9) Miller, J. A.; Klippenstein, S. J. *J. Phys. Chem. A* **2003**, *107*, 7783–7799.
- (10) Dagaut, P.; Cathonnet, M. *Combust. Flame* **1998**, *113*, 620–623.
- (11) Li, Y.; Zhang, L.; Tian, Z.; Yuan, T.; Zhang, K.; Yang, B.; Qi, F. *Proc. Combust. Inst.* **2009**, *32*, 1293–1300.
- (12) McEnally, C. S.; Pfefferle, L. D.; Robinson, A. G.; Zwier, T. S. *Combust. Flame* **2000**, *123*, 344–357.
- (13) Richter, H.; Howard, J. B. *Phys. Chem. Chem. Phys.* **2002**, *4*, 2038–2055.
- (14) Frenklach, M. *Phys. Chem. Chem. Phys.* **2002**, *4*, 2028–2037.
- (15) Baird, W. M.; Hooven, L. A.; Mahadevan, B. *Environ. Mol. Mutagen.* **2005**, *45*, 106–114.
- (16) Finlayson-Pitts, B. J.; Pitts, J. N., Jr. *Science* **1997**, *276*, 1045–1052.
- (17) Kazakov, A.; Frenklach, M. *Combust. Flame* **1998**, *112*, 270–274.
- (18) Gu, X.; Zhang, F.; Guo, Y.; Kaiser, R. I. *Angew. Chem., Int. Ed.* **2007**, *46*, 6866–6869.
- (19) Glassman, I., Ed. In *Combustion*, 3rd ed.; Academic Press: New York, 1996.
- (20) Barckholtz, C.; Fadden, M. J.; Hadad, C. M. *J. Phys. Chem. A* **1999**, *103*, 8108–8117.
- (21) Lin, M. C.; Mebel, A. M. *J. Phys. Org. Chem.* **1995**, *8*, 407–420.
- (22) Mebel, A. M.; Lin, M. C. *J. Am. Chem. Soc.* **1994**, *116*, 9577–9584.
- (23) Tokmakov, I. V.; Kim, G.-S.; Kislov, V. V.; Mebel, A. M.; Lin, M. C. *J. Phys. Chem.* **2005**, *109*, 6114–6127.
- (24) Albert, D. R.; Davis, H. F. *J. Phys. Chem. Lett.* **2010**, *1*, 1107–1111.
- (25) Gu, X.; Zhang, F.; Kaiser, R. I. *Chem. Phys. Lett.* **2007**, *448*, 7–10.
- (26) Gu, X.; Guo, Y.; Zhang, F.; Mebel, A. M.; Kaiser, R. I. *Faraday Discuss.* **2006**, *133*, 245–275.
- (27) Mallard, W. G.; Linstrom, P. J. *NIST Chemistry WebBook*; National Institute of Standards and Technology: Gaithersburg, MD, 2000.
- (28) Gu, X. B.; Guo, Y.; Kawamura, E.; Kaiser, R. I. *Rev. Sci. Instrum.* **2005**, *76*, 083115/083111–083115/083116.
- (29) Guo, Y.; Gu, X.; Kawamura, E.; Kaiser, R. I. *Rev. Sci. Instrum.* **2006**, *77*, 034701/034701–034701/034709.
- (30) Vernon, M. *Ph.D. Thesis*, University of California, Berkeley, 1981.
- (31) Weis, M. S. *Ph.D. Thesis*, University of California, Berkeley, 1986.
- (32) Levine, R. D. *Molecular Reaction Dynamics*; Cambridge University Press: Cambridge, UK, 2005.
- (33) Davis, H. F. *personal communication*, 2011.